LA-UR 94-3546

Los Alamos National Laboratory is operated by the University of California for the United States Department of Energy under contract W-7405-ENG-36

TITLE: **Level Set Techniques Applied to Unsteady Detonation Propagation**

AUTHOR(S): **John B. Bdzil, Tariq Aslam, Jin Yao, D. Scott Stewart**

SUBMITTED TO: **Mathematical Modeling & Combustion Science, Kauai, Hawaii July 18-22, 1994**

DISCLAIMER

Los Alamos National Laboratory
Los Alamos, New Mexico 87545

Level Set Techniques Applied to Unsteady Detonation Propagation

D. Scott Stewart[1] *Tariq Aslam*[1] *Jin Yao*[1] *and John B. Bdzil*[2]

[1] Theoretical and Applied Mechanics
University of Illinois, Urbana, Illinois, 61801, USA
[2] Los Alamos National Laboratory, Los Alamos, New Mexico, 87545, USA

1 Introduction

TO ALL AUTHORS: This a FIRST COMPLETE DRAFT ... and is still being written, there are probably errors and inconsistencies. We cannot add much text if any. 1. Please proof read carefully, especially parts that you are most familiar, responsible for 2. Check the logic of everything that you read 3. Check prose commas etc., 4. Check figure captions and suggest revisions, 5. Check references 6. Suggest places to cut text. First revisions must be given to me by Monday. The due date is Thursday Scott

Here we are concerned with describing the dynamics of multidimensional detonation as a self-propagating surface. The detonation shock surface has been shown under certain circumstance to be governed by an intrinsic relation between the normal shock velocity and the local curvature, obtaining a $D_n - \kappa$ relation. Once the initial shock position is given, then subsequently the motion of the shock can be determined by solving a scalar partial differential equation for the shock position. One can think that in principle, the $D_n - \kappa$ relation is determined by some means, theory or experiment, and then once prescribed, predictions of the physical system further depend wholly on the initial configuration. Thus we are also concerned about an efficient numerical solution of this equation in three-dimensions, with possibly multiply connected and disjoint shock surfaces. This has led us to consider the level-set techniques of Osher and Sethian [1], which are naturally suited to these problems.

In what follows, we discuss examples of propagating surfaces, from formulations in combustion and heat transfer to which level-set methods apply. In Sect. 3. we discuss the specific example from detonation theory, which summarizes our recent work in [2]. In Sect 4. we briefly explain the derivation of the $D_n - \kappa$ relation, in the context of detonation and mention some recent extensions of the theory, that includes shock acceleration terms and the possibility of extinction for reaction rates that have large activation energies [3]. These new results can all be summarized as an extension of the $D_n - \kappa$ relation, to a relation of the form $F(\dot{D}_n, D_{n,t}, \kappa) = 0$ where $\dot{D}_n$ is the acceleration of the detonation shock along its normal. Importantly, the resulting equation is hyperbolic in character as opposed to parabolic, for a simple $D_n - \kappa$ relation. Finally we indicate the interesting new features of the dynamics that can be observed in the detonation shock surface evolution, and speculate on their relevance to formation of sustained detonation cells.

2 Examples of Propagating Surfaces

Theory for propagating surfaces arise naturally from discussion of phase transformation, that involve a change in enthalpy. Examples include solidification and the Stefan problem, flame propagation and detonation propagation. In the first case the surface is the boundary between solid and liquid, in the second case the flame surface, in the last case the detonation shock surface. In all three cases, the actual surface is not a material surface, but a phase surface through which material passes. The surface is assumed separate the two phase (for arguments sake, unburnt and burnt), and the normal unit vector is defined to be positive in the direction of the unburnt material. At each point on the surface the normal velocity is designated D_n and the local total curvature (the sum of the principle curvature) is designated by κ. Further κ is assumed to be positive when the surface is convex, relative to a normal pointing towards the unburnt material.

Next we delineate between two types of propagating surfaces, *Not Self-Propagating Surface (NSPS)* and *Self-Propagating Surface (SPS)*. We distinguish these two cases as follows. We define a surface that is *Not Self-Propagating* to be one that requires information normal to the surface to define the normal velocity D_n. So for an NSPS one includes relations of the form $D_n = F(\kappa, \mathbf{x}, t, n_+)$, where F generally depends on the curvature, the spatial position of the wave, time and the values of quantities on one side (here the burnt side) of the surface. The slowly varying hydrodynamical limit of a flame, described in [4], is an excellent example of an NSPS.

In contrast, we define a *Self-Propagating Surface* that only requires information defined in the surface to determine normal velocity D_n. So for an SNPS one has a relations of the form $D_n = F(\kappa, \mathbf{x}, t,)$, or $D_n = F(\kappa, \mathbf{x}, t, \dot{D}_n)$,where F generally depends on the curvature, the spatial position of the wave, time and possibly the self-acceleration of the surface, in its normal direction. Examples of SPS with D_n of the form $D_n = F(\kappa)$ include the simple Markstein flame, [5], or the simplest version of the $D_n - \kappa$ relation obtained from Detonation Shock Dynamics; $D_n = D_{CJ} - \alpha\kappa$, where D_{CJ} and α are positive constants. As we mention in Sect. 3 the acceleration term $\dot{D}_n$ also arises naturally in the description of weakly curved detonation and enlarges the dynamics that is considered in the DSD-theory.

need to re-write here on the form of the relation, f(dndot,dn,kappa) = 0 (say)

3 Level Set Methods: Tools for Computing the Dynamics of Interfaces

Here we would like to outline the level-set method and explain its application and usefulness as a tool for computing the dynamics of propagating interfaces. The first point is to notice that a interface (or surface) is a subset of lower dimensionality than the space that it travels in. The level-set technique solves for a field function $\psi(\mathbf{x}, t)$ that depends on position in physical space and time, and the field identifies surfaces of constant values of ψ. The surfaces $\psi(\mathbf{x}, t) = 0$, is

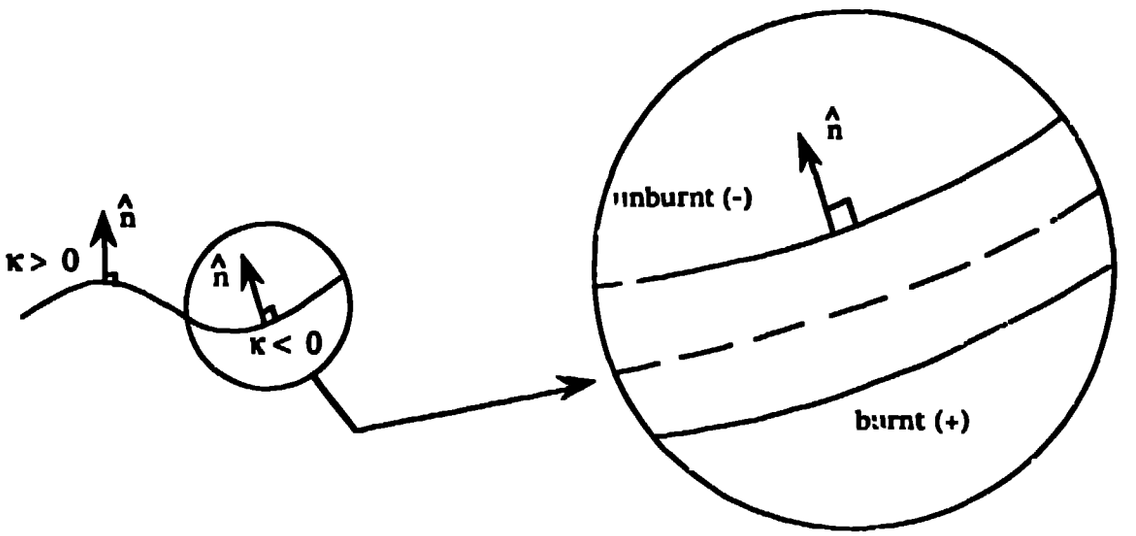

Fig. 1. Schematic of a propagating surface. The outward normal points toward "unreacted" material. The blow up indicates a layer, within the structure of the surface that is has physics that may control its propagation, like a reaction zone.

typically identified with the surface of physical interest. Therefore the computational task involves computing a field in space- time. One then exhibits the surface of interest by searching for the special surface $\psi = 0$.

This imbedding method is in contrast to what are sometimes known as *surface methods*, where one represents the surface of physical interest by a representation of the same dimension. For example, in two-dimensions, the detonation shock locus is a space-curve in the (x,y)-plane and a numerical discretization represents the shock as a 1D array. For a 3D application the shock surface is a 2D space-surface and the discretization is represented by a 2D array. Differential representations of the surface, are based on surface parameterizations. The discrete representations of the surface often include marker particles in the surface, or finite elements.

While numerical methods based on surface parameterization can be very effective for many problems and can yield results with high accuracy, they also have substantial numerical and logical problems, as the geometric complexity of the underlying problem increases. If the surface rapidly expands or contracts, markers must be added or removed. Surface markers can cross and the stability and accuracy of the method can be lost. The logical complexity of the programming, for a surface parameterization method can be overwhelming if one considers problems that have surfaces that are disjoint or multiply connected.

It might seem that additional computation is required for the level-set techniques, since they solve for a field in the dimension of the physical space, one compensates for that by using an efficient, high-accuracy numerical method, that is logically simple to program; a point that was made dramatically in Osher and

Sethian's 1988 paper, [1]. Certainly we have found, so far for our applications, the advantages of the logical simplicity of implementation of the level-set methods, easily compensates for any perceived increase in computational cost due to working in a higher dimension .

3.1 Detonation Shock Dynamics

Detonation Shock Dynamics (DSD) is a name that we use to describe a collection of results of an asymptotic theory describes the evolution of a multi-dimensional, curved detonation. The detonation shock is supported by a combustion reaction zone that trails behind the shock, and the radius of curvature of the detonation shock is assumed to be large, compared to the reaction zone thickness. Most of the results, [6], [7], [8], that have been developed so far, assume that the speed of the detonation was close to its, plane, Chapman-Jouguet, (CJ) value. In particular, the theoretical results give explicit expressions for the $D_n - \kappa$ relation for an explosive material, described by the Euler equations, with a specified equation of state and reaction rate law. The work mentioned in [3], and in Sect. 4, extends this to include $\dot{D}_n$.

The theory of DSD suggest that detonation shock, in some regimes, propagate according to a material specific evolution law. This theoretical suggestion has provided the motivation to verify this assertion experimentally in explosive systems. Fig. 2., shows a facsimile of the experimentally determined $D_n - \kappa$ curve for a condensed explosive PBX9502. For positive curvature, the experiments were conducted by Davis and Bdzil of Los Alamos National Laboratory, [9], and for those of negative curvature, the experiments were conducted by Hull of LANL, [10]. The two sets of experiment were carried out in quite different geometries; Davis and Bdzil's experiments were for round sticks of explosive of different diameters, ignited at the bottom, while Hull's experiments were generated by an entirely different sort of experiment, where two, separated point detonations were ignited far within a block of the explosive and the waves then eventually merged to form a single detonation shock. Importantly the combined data of the two separate experiments, show the value for the detonation velocity at zero curvature, and have the same slope where they join.

The Bdzil-Davis reduction of the experimental data for PBX9502, for the positive curvature side, also indicates the possibility of an extinction point; defined here as a maximum value of positive curvature, beyond which the $D_n - \kappa$ relation may not be continued. Under certain assumption, theory also shows a similar property for $D_n - \kappa$ curves.

Without further explanation or assumption in this section, we will assume that we have a $D_n - \kappa$ relation that will describe the motion of a detonation shock for some range of normal velocities and curvature, such as the ones mentioned above. Further for simplification of the presentation, let's use D_{CJ} to scale the velocity, so that scaled $D_{CJ} = 1$. A $D_n - \kappa$ relation then can be assumed to have the form

$$D_n = 1 - \alpha(\kappa), \tag{1}$$

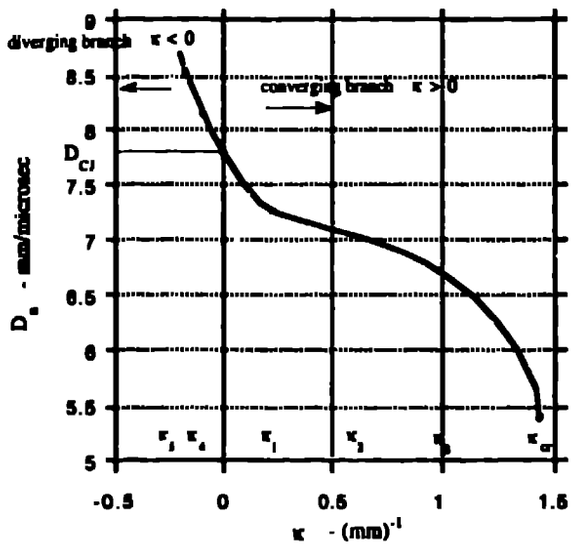

Fig. 2. Calibrated $D_n - \kappa$ response of condensed explosive PBX 9502

and some other simple remerks are in order. The $D_n - \kappa$ relation based on intrinsic description corresponds to a SPS, in the sense define in Sect. 2.. If $\alpha = 0$, one is lead to a Huygens' construction for the motion of the shock surface. In the presence of non zero α, one can propagate the surface by a modified Huygen's construction. If D_n is a monotonically decreasing function of the curvature, then the underlying dynamics of the surface are those of a parabolic partial differential equation. Indeed under certain assumption the shock slope of the shock surface can be show to obey Burger's equation.

3.2 Level-Set Formulation

Next we turn to the level-set technique as a way to solve for the motion of the surface, given this specific example of DSD. It is assumed that there is a field $\psi(x, y, z, t)$ that will define level surfaces of the form, $\psi(x, y, z, t) = constant$. The *shock* location for all time, will be defined as the special surface $\psi(x, y, z, t) = 0$. The initial location of the shock with be associated with the locus $\psi(x, y, z, 0) = 0$.

The ψ function obeys the *level-set equation* which is derived as follows. On any level curve $\psi(x, y, z, t) = constant$, the time derivative of ψ in a frame, travelling in that surface is zero, i.e.

$$\frac{d\psi}{dt} = \frac{\partial\psi}{\partial t} + \frac{d\mathbf{x}}{dt} \cdot \nabla\psi = 0, \tag{2}$$

where the derivative $d\mathbf{x}/dt \equiv \mathbf{D}$, is the pointwise velocity of the surface. By using the definition of the normal to the constant $\hat{n} = \nabla\psi/|\nabla\psi|$ and noticing that $\mathbf{D} \cdot \nabla\psi$ can be rewritten as $D_n|\nabla\psi|$, the above equation, now referred to as the level-set equation, can be restated as

$$\frac{\partial\psi}{\partial t} + \mathbf{D}_n \cdot |\nabla\psi| = 0. \tag{3}$$

If D_n is a constant, then the level-set equation is a Hamilton-Jacobi equation. If D_n is a function of the curvature, then the level-set equation is a Hamilton-Jacobi like equation. Importantly, the type of the equation is controlled by the highest order derivative that appears. For example in the current context, if D_n is a monotonically decreasing function of the curvature, then the level-set equation is at most first order in time, is second order in space, and can be classified as a parabolic partial differential equation (PDE).

To illustrate the level-set PDE more completely, in the form used for DSD applications, one need the Cartesian expression for the curvature. The curvature is generally represented as $\kappa = \nabla \cdot \hat{n}$, which In two-dimensions reduces to

$$\kappa = \frac{\psi_{xx}\psi_y^2 - 2\psi_{xy}\psi_x\psi_y + \psi_{yy}\psi_x^2}{\left(\psi_x^2 + \psi_y^2\right)^{3/2}}. \tag{4}$$

The partial differential equation for ψ in a Cartesian frame, wholly prescribed once the function $D_n(\kappa)$ is given. The initial data for ψ can be generated as follows. At time $t = 0$, define $\psi(x, y, z, 0) = 0$ to be the same as the initial shock position. Note that one could have more than one closed surface identifying initial shocks. Then the remainder of the initial data for the field can be defined by setting the value of ψ at any point (x,y,z) equal to the minimum distance to the detonation shock. Fig. 3 shows an example of the level-set function ψ defined intitially (as the minimum distance function) and at a later time, for the example of two cylindrically expanding shocks that are at first seperated and then merge.

The numerical solution of the PDE with initial and boundary conditions, which we will mention next, generates an approximation to the field $\psi(x, y, z, t)$, in general and the location of the shock is then simply found by search for the level surface $\psi = 0$. This is easily done by creating a table of crossing times of the shock across the computational node. We call this the crossing table. The crossing table is created by testing the sign of the level set function at each computational node at each time-step, and then recording the time(s) when the level set function changes sign. A tabular function of the form $t_{cross}(x, y, z)$ is found from the computation. The shock location at given time is simply a contour of constant time.

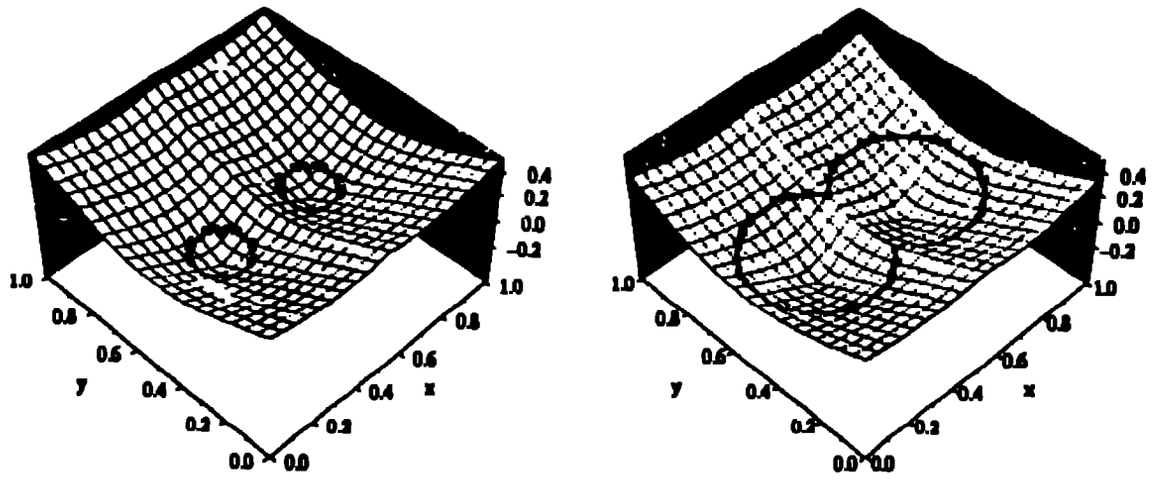

Fig. 3. The level-set function ψ defined intitially (as the miminimum distance function) and at a later time, for the example of two cylindrically expanding shocks that are at first seperated and then merge.

3.3 Boundary Conditions

Here we give only the briefest of summary of the boundary conditions that are applied in the DSD application. A detailed description of the boundary conditions and there rationale is found in [2]. The need for boundary conditions comes from the application. The problems of interest in explosive design, mostly involve domains of finite size, and the collision of the detonation shock with confinement boundaries. In typical explosive systems, one places the unreacted explosive in a container. After having been ignited, the detonation sweeps through the system and the detonation shock intersects interfaces. Often the confinement is a thin layer of metal which then seperates the explosive products from the ambient atmosphere.

The boundary conditions that have been considered so far, are motivated by analysis that model the interaction of the detonation shock with the confinement boundary, and fall into three simple categories i) shock-edge angle boundary conditions, ii) reflective boundary conditions, and iii) continuation boundary conditions. The shock-edge boundary condition was put forward by Bdzil in [11], and used later in [6], and says that in certain instances, the angle that the shock makes with the Interface is a fixed, and that fixed angle is a material constant for an explosive-confining material pair. Let the normal of the detonation shock at the edge be represented as $\hat{n}_{edge}$ and let the outward normal of the interface, where the detonation shock and the Interface intersect, be represented as $\hat{n}_{mat}$, then the interior angle between those two direction vectors is some fixed value $\omega = \omega_c$. For example, the angle for a PBX9502 explosive with Copper confining material, of some specified thickness, is a fixed number; a typical value is 45 degrees.

The reflective boundary condition is that the detonation is normal to the interface, hence ω is equal to 90 degrees. Finally the continuation boundary condition is used in certain circumstances, if the detonation wave is highly oblique to the interface and the interior angle ω is close to zero. Then the detonation shock would be so fast relative to the confinement edge, that the reaction zone would not be influenced by the boundary. In this case, no boundary condition is applied at all. Continuation means that the the detonation shock is extended beyond the boundary as a smooth interpolant, as needed to determine the numerical solution, but no angle boundary condition is applied.

In practice, for a DSD explosive application, all three of these boundary condition might be applied according to the interior angle ω that is realized at the edge interface. One of the most important points to stress, is that all of the boundary conditions, described above are at most function of the derivatives of ψ. Thus a level curve propagated, according to the $D_n - \kappa$ relation, will evolve only according to data developed in its own surface. The boundary condition that are considered for the DSD applications do not change this property and thus one is lead to a class of problems in finite domains that can be solved consistently using level-set techniques.

3.4 The recipe for DSD Application Using Level-Set Methods

The recipe for using level set methods for the DSD application can then be summarized in a simple way as follows. 1) Determine the initial detonation shock locations and designate them as $\psi(x, y, z, 0) = 0$. 2) Define the ψ field everywhere at time $t = 0$ say, by setting ψ equal to the minimum distance to the detonation shock (say). 3) Solve the level- set equation for the ψ field. 4) At the boundary, apply the boundary condition for each level curve, as if it were the physical shock of interest. 5) The physical shock at any time of interest is found by searching for $\psi(x, y, z, t) = 0$.

3.5 The Numerical Methods

Here we give a brief description of a general numerical method for solving the level-set equation for the DSD application, on a fixed Eulerian finite difference grid. For the interior algorithm, we follow Osher and Sethian, [1]. The normal velocity D_n is explicity written as $D_{CJ} - \alpha(\kappa)$, where if the second term was absent, then one solves only the Huygen's construction. The update of ψ is split into a Huygen's advection followed by a diffusive correction. The Huygen's advection uses a second order ENO scheme. The diffusive correction, due to the curvature terms in $\alpha(\kappa)$ are approximated by central differencing. The boundary condition are implement with central differences and are second order accurate. The reader is referred to [2] for more details. Suffice it to say that the advantage of the ENO-based schemes for the advection is the simplicity of implementation and accuracy of results.

4 Asymptotic Theory

Here we summarize the asymptotic theory that is developed in [3], and which includes new terms. A standard mathematical model of explosive materials is adopted, comprised of the compressible Euler equations for an ideal equation of state, and Arrhenius form for the reaction rate r,

$$e = \frac{p}{\rho}\frac{1}{\gamma - 1} - Q\lambda, \quad r(p, \rho, \lambda) = k(1-\lambda)^{\nu} e^{-E/(p/\rho)}, \tag{5}$$

where e is the specific internal energy, ρ is the density, p is the pressure, λ is the reaction progress variable, γ is the polytropic exponent, Q is the heat of combustion and k, ν and E are respectively the premultiplying rate constant, the depletion factor and the activation energy. The velocity will be represented by u. Further, from here on, we adopt the notation convention where a quantity with a $\tilde{()}$ refers to a dimensional quantity and the quantities without a tilde are dimensionless quantities that are scaled with respect to the dimensional unit. In particular the length, velocity and time scales are given by $\tilde{\ell}_{rz}, \tilde{D}_{CJ}$ and $\tilde{\ell}_{rz}/\tilde{D}_{CJ}$ respectively. The length $\tilde{\ell}_{rz}$, is taken to be a characteristic 1D, steady reaction zone length. The pressure density scale is $\tilde{\rho}_0$ and pressure scale is $\tilde{\rho}_0\tilde{D}_{CJ}^2$. Consequently the sound speed, reaction rate, curvature and heat of combustion appear as $c = \tilde{c}/\tilde{D}_{CJ}$, $r = \tilde{r}\tilde{\ell}_{rz}/\tilde{D}_{CJ}$, $\kappa = \tilde{\kappa}\tilde{\ell}_{rz}$, $q = \tilde{Q}/\tilde{D}_{CJ}^2 - 1/(2(\gamma^2-1))$.

The jumps across the lead detonation shock are determine by the equation of state and the upstream state. We will assume that the upstream state is quiescent with $u = 0$, density ρ_0 and ambient pressure p_0. For convenience, we will assume that the lead detonation shock is sufficiently strong so that the strong shock approximation, holds. The normal shock relations for an ideal gas moving into an ambient atmosphere, reduce to

$$U_n = -\frac{\gamma-1}{\gamma+1}D_n, \quad u_t = 0, \quad \rho = \frac{\gamma+1}{\gamma-1}, \quad p = \frac{2}{\gamma+1}D_n^2, \quad \lambda = 0, \quad \text{at } n = 0. \tag{6}$$

where the $n-$ and $t-$ subscripts respectively refer to the normal component of the shock velocity and the tangential component(s) as defined by the shock normal. Also for the strong shock approximation, the plane, steady, CJ detonation velocity is given by $D_{CJ}^2 = 2(\gamma^2-1)Q$.

4.1 Intrinsic, Shock-Attached Coordinates and governing equations

In order to make the analysis tractable, it is essential to write the equations of motion in a suitable form. Given that the material derivative is given by $D/Dt \equiv \partial/\partial t + \mathbf{u}\cdot\nabla$, then the Euler equations, with reaction, are given by $D\rho/Dt + \rho\nabla\cdot\mathbf{u} = 0$, $\rho\, D\mathbf{u}/Dt + \nabla p = 0$, $De/Dt + p\, Dv/Dt = 0$, where $v \equiv 1/\rho$ and $D\lambda/Dt = r(p, \rho, \lambda)$.

Intrinsic, shock-attached coordinates, are used to describe curved, time-evolving detonation waves. We restrict the formulas shown here to 2D to simplify the presentation, only. The shock surface that can be represented quite generally

In terms of laboratory-fixed coordinates (x, y) by a function $\psi(x, y, t) = 0$. This equation constrains the lab-coordinate position vectors in the surface to $\mathbf{x} = \mathbf{x}_s(x, y, t)$. The shock surface can also be represented by a surface parameterization $\mathbf{x} = \mathbf{x}_s(\xi, t)$, where ξ measures length along the coordinate lines of the surface. The outward normal (in the direction of the unreacted explosive) and unit tangent vector in the shock surface, (which form a local basis) are given by $\hat{n} = \nabla\psi/|\nabla\psi|$, $\hat{t} = \partial\mathbf{x}_s/\partial\xi$. The total shock curvature is given by $\kappa(\xi, t) = \nabla \cdot \hat{n}$. Finally, the intrinsic coordinates are related to the laboratory coordinates by the change of variable given by $\mathbf{x} = \mathbf{x}_s(\xi, t) + n\,\hat{n}(\xi; t)$, where the variables n, ξ are respectively the distance measured in the direction of the normal to the shock wave, and the arclength measured in the shock surface along the principle lines of curvature.

Next the equations of motion are transformed to this shock-attached, intrinsic frame, i.e. from (x,y,t)-coordinates to (n, ξ, t) coordinates. In particular we note, that the normal shock velocity and curvature are only function of ξ and t, i.e. $D_n = D_n(\xi, t)$ and $\kappa = \kappa(\xi, t)$. The relevant normal velocity that appears subsequently is $U_n = u_n - D_n$. The manipulations of the transformation are lengthy but straightforward and the transformed equations have a direct correspondence to the Euler equations. Importantly, the curvature appears explicitly in the transformed equations.

For the transformed equations, we retain only the explicit time dependence and the first curvature effects and write down a set of approximate equations to analyze that are valid under the assumption that $|\kappa| << 1$. Consistent with the normal shock relations, for a shock propagating into a quiescent material, we neglect u_ξ in this analysis and take it effectively to be zero. The equations are then written in a a quasi- conservative form as

$$\frac{\partial(\rho U_n)}{\partial n} = -\kappa\rho(U_n + D_n) - \rho_{,t}, \tag{7}$$

$$\frac{\partial(\rho U_n^2 + p)}{\partial n} = -\rho_{,t}U_n - \kappa\rho U_n(U_n + D_n) - \rho(U_{n,t} + D_{n,t}), \tag{8}$$

$$\begin{aligned}\frac{\partial}{\partial n}\left(\frac{1}{2}U_n^2 + \frac{1}{\gamma - 1}c^2 - q\lambda\right) &= -(U_{n,t} + D_{n,t}) \\ &\quad -\frac{1}{U_n}\left(\frac{1}{\gamma - 1}\frac{p_{,t}}{\rho} - \gamma\frac{p}{\rho^2}\frac{\rho_{,t}}{\gamma - 1} - q\lambda, t\right).\end{aligned} \tag{9}$$

The rate equation can be written as

$$\frac{\partial\lambda}{\partial n} = \frac{i}{U_n}(r - \lambda_{,t}), \tag{10}$$

An auxiliary equation, referred to as the *master equation* can be written

$$(c^2 - U_n^2)\frac{\partial U_n}{\partial n} = qr(\gamma - 1) - \kappa c^2(U_n + D_n) + U_n(U_{n,t} + D_{n,t}) - \frac{p_{,t}}{\rho}. \tag{11}$$

Note that for the equations listed above, $()_{,t} = \partial/\partial t|_{(n,\xi)}$.

The analysis proceeds the assumption that the left-hand side of the structure equations (7) - (10) are in some sense uniformly small and can be approximated by a quasi-steady, plane solution. One applies the shock boundary conditions, (6) at $n = 0$ and attempts to generate a uniform solution throughout the reaction zone behind the shock.

4.2 The Generalized CJ Conditions

The master equation (11) exhibits the special character of the sonic point that generates a condition that can be used, under appropriate circumstances, to generate the eigenvalue relation between curvature and the normal detonation speed, and the self-acceleration.

Suppose the flow has a sonic point that

$$\eta = c^2 - U_n^2 = 0, \tag{12}$$

then equation (11) is satisfied at that point, in general, only if, the right hand side, vanishes simultaneously at that point, i.e.

$$q\tau(\gamma - 1) - \kappa c^2(U_n + D_n(t)) + U_n(U_{n,t} + D_{n,t}) - vp_{,t} = 0. \tag{13}$$

The pair of conditions (12, 13) are called the sonic and the thermicity conditions repectively, and taken together are called the "generalized CJ-conditions", after Wood and Kirkwood, [13].

4.3 The Method of Successive Approximation

The problem outlined above, for quasi-steady, near-CJ, curved detonation, in the absence of explicit time-dependent terms, has been solved by a layer analysis, in [6], [7], [13], [8]. However in [3] we have used a technique, that is equivalent and perhaps simpler, and is based on an integral formulation rather than differential equations.

For the purpose of generating the corrections we assume that the detonation velocity and the state corresponds to a quasi-steady, 1D solution, plus a correction,

$$D_n = D + \kappa D' \tag{14}$$

and

$$U_n = -D\frac{\gamma - \ell}{\gamma + 1} + \kappa U', \quad v = \frac{\gamma - \ell}{\gamma + 1} + \kappa v', \quad p = D^2\frac{1 + \ell}{\gamma + 1} + \kappa p', \tag{15}$$

where $\ell = \sqrt{1 - \lambda/D^2}$. To keep notation to a minimum, a * subscript to refer to the first approximation for the fluid state and a prime superscript is association with the correction to that approximation, e.g., $U_n = U_*(\ell, D) + \kappa U'$. We represent the leading order approximation to D_n, $(D_r)_*$, where it would

appear by a plain D. All that is assumed for now, in the various expansions (illustrated by the expansion for U_n is that the correction term $:U' \sim o(U)$ as $\kappa \to 0$. The resulting integral equations, have been further simplified by using the first approximation in the integrals. Finally we also use the rate equation (10) to change the independent variable of integration from n to the progress variable λ to obtain equations for the approximations of ρ, U_n, p and D_n, satisfy

might need some more explanation on the expansions here

$$\rho U_n + D_n(t) = \int_0^\lambda [-\kappa\rho_*(U_* + D) - \rho_{*,t}]\frac{U_*}{r_*}d\bar{\lambda}, \tag{16}$$

$$\rho U_n^2 + p - D_n^2(t) = -\int_0^\lambda [(\rho_* - 1)D_{,t} - \kappa D(U_* + D)]\frac{U_*}{r_*}d\bar{\lambda}, \tag{17}$$

$$\frac{1}{2}U_n^2 + \frac{c^2}{\gamma - 1} - q\lambda - \frac{1}{2}D_n^2(t) = \int_0^\lambda [-\frac{p_{*,t}}{D} - (1 + \frac{D}{U_*})D_{,t}]\frac{U_*}{r_*}d\bar{\lambda}. \tag{18}$$

In particular, one can evalute the corrected state at the CJ-point, where setting $\lambda = \lambda_{CJ}$, to obtain an approximation to the state there. The resulting formulas represent a correction of the RH jump relations for the state at the generalized-CJ point.

$$(\rho U_n)_{CJ} = -D_n + \kappa I_1 D^2 + J_1 D_{,t}, \tag{19}$$

$$(\rho U_n^2)_{CJ} + p_{CJ} = {D_n}^2 - \kappa I_2 D^3 + I_1 D D_{,t}, \tag{20}$$

$$\frac{1}{2}(U_n^2)_{CJ} + \frac{c_{CJ}^2}{\gamma - 1} - q\lambda_{CJ} = \frac{{D_n}^2}{2} - (I_1 + J_2)D D_{,t}, \tag{21}$$

where the reaction rate integrals I_1, I_2, J_1, J_2 are defined by

$$I_1 = \frac{1}{(\gamma + 1)}\int_0^{\lambda_{CJ}} \frac{(1 + \ell)}{r}d\lambda, \quad I_2 = \frac{1}{(\gamma + 1)^2}\int_0^{\lambda_{CJ}} [\frac{(\gamma - \ell)(1 + \ell)}{r}]d\lambda, \tag{22}$$

$$I_3 = \frac{1}{(\gamma + 1)^2}\int_0^{\lambda_{CJ}} \frac{\ell(\gamma - \ell)}{r}d\lambda, \quad I_4 = \int_0^{\lambda_{CJ}} \frac{\ell}{r}d\lambda, \tag{23}$$

$$J_1 = \frac{1}{\gamma}\frac{d(DI_4)}{dD}, \quad J_2 = -\frac{1}{D^2}\frac{d(D^3 I_3)}{dD}. \tag{24}$$

The formal algebraic solution of equations (19) - (21) subject to the sonic constraint that $c^2 = U_n^2$, in fact determines the state $\rho_{CJ}, (U_n)_{CJ}, p_{CJ}$ and a condition on the speed D_n, in the same way as is obtained for the simplest case of a steady, plane, CJ wave. The result for U_n, and the sonic condition $c^2 = U_n^2$ can then be used in the remaining equation (21) to obtain condition on D_n, which in fact is a condition on $D_{,t}, D_n, \kappa$ and λ_{CJ},

$$D_n^2 - \lambda_{CJ} + \gamma^2 \left\{ \frac{[D_n^2 - \kappa I_2 D^3 + I_1 D D_{,t}]^2}{[D_n - \kappa I_1 D^2 - J_1 D_{,t}]^2} - D_n^2 \right\} + 2(\gamma^2 - 1)(I_1 + J_2) D D_{,t} = 0. \quad (25)$$

which can be further simplfied by retaining only the first correction in $O(\kappa)$ and $O(D_{,t})$, which are assumed small to obtain the reduced $(D_{,t}, D_n, \kappa, \lambda_{CJ})$ relation

$$D_n^2 - \lambda_{CJ} + 2\kappa\gamma^2(I_1 - I_2)D^3 + 2DD_{,t}[(\gamma^2 - 1)(I_1 + J_2) + \gamma^2(I_1 + J_1)] = 0. \quad (26)$$

where we have replaced D by D_n and $D_{,t}$ by $\dot{D}_n$.

In most respects, equation (26) is the key result and holds generally for slowly varying, weakly curved detonation structure that has a sonic character. The evolution equation is obtained once λ_{CJ} is estimated, which follows from consideration of the thermicity condition., (13).

4.4 Large Activation Energy

In the general case, the quantities, I_1, I_2, J_1 and J_2 are functions of D_n and $\dot{D}_n$, thus it is generally difficult to write down the $\dot{D}_n, D_n, \kappa$- relation in very simple terms. For the purpose of illustration, we focus on the case of large activation energy, which follows our work in [8]. In this case, the reaction zone structure is assumed to be that of an induction zone, followed by an exponentially thin reaction zone. It follows that we can assume that λ_{CJ} is exponentially close to one. Further we assume that D_n is close to one, and that quasi-steady time variation in the induction zone is due to the motion of the shock, and that $\dot{D}_n$ and κ are small and of the same order. Equation (26) can be further simplified to

$$D_n = 1 - \gamma^2(I_1 - I_2)\kappa - (\gamma^2(I_1 + J_1) + (\gamma^2 - 1)(I_1 + J_2))\dot{D}_n \quad (27)$$

The characteristic reaction zone length is estimated in terms of the induction zone length scale, $\tilde{\ell}_{rz} = \tilde{k}^{-1}\tilde{D}_{CJ}exp[\theta/c_s^2]/\theta$ and thus the reaction rate is expressed as

$$r = \frac{(1-\lambda)^\nu}{\theta} e^{\theta/c_s^2 - \theta/c^2}. \quad (28)$$

For $\gamma < 2$, the rate term is exponentially large outside the induction zone, hence the values of the rate integrals I_1, I_2, J_1, J_2 only depend on their behavior in the induction zone.

Consideration of the induction zone then allows for calculation of the temperature (sound speed squared) perturbation in the zone, in terms of the curvature and the slow acceleration of the detonation and small depletion, and obtains the estimate for c^2,

$$c^2 = c_s^2 + \alpha\lambda + \frac{c_s^4}{\theta}\ln\left\{\frac{\theta\kappa\beta}{\alpha}\left(1 - e^{-\alpha\lambda\theta/c_s^4}\right) + exp[\frac{(\gamma+1)^2}{\gamma(\gamma-1)}\theta(D_n - 1)]\right\}. \quad (29)$$

where $c_s^2 = [2\gamma(\gamma-1)]/(\gamma+1)^2$ and

$$\alpha = \frac{\gamma(3-\gamma)}{2(\gamma+1)^2}, \quad \kappa\beta = 4\left(\frac{\gamma(\gamma-1)^3}{(\gamma+1)^4}\kappa + 2\frac{\gamma(\gamma-1)(\gamma-2)}{(\gamma+1)^3}\frac{\dot{D}_n}{\theta}\right). \quad (30)$$

All that remains is the integral asymptotics, which can be summarized as follows. For large θ, the dominant contributions to the integrals are close to the shock, where $\ell = 1$, and it follows that $J_1 \sim 0$ and $I_1(\gamma+1)/2 \sim (I_1 - I_2)(\gamma+1)^2/4 \sim -J_2(\gamma+1)^2/[4(\gamma^2-1)] \sim I$, where

$$I = \int_0^1 \frac{1}{r}d\lambda \sim \int_0^\infty e^{-\theta(c^2-c_s^2)/c_s^4}dz \text{ where. } z = \lambda\theta, \quad (31)$$

In turn, I can be estimated using the approximation for c^2 in the reaction rate r, as

$$I = \frac{c_s^4}{\theta\kappa\beta}[\ell n(\sigma) - \ell n(\sigma - \theta\kappa\frac{\beta}{\alpha})]. \quad (32)$$

where

$$\sigma - \theta\frac{\kappa\beta}{\alpha} = exp\left(\frac{(\gamma+1)^2}{\gamma(\gamma-1)}\theta(D_n - 1)\right). \quad (33)$$

Now we substitute these various results back into (27) to obtain

$$\kappa = \frac{\alpha}{\beta\theta}e^{2/c_s^2 - \beta/\mu)\theta(D_n-1)}(1 - e^{(\beta/\mu)\theta(D_n-1)}). \quad (34)$$

where

$$\kappa\mu = c_s^4[\frac{4\gamma^2}{(\gamma+1)^2}\kappa + \frac{2\gamma(4\gamma-3)}{\gamma+1}\frac{\dot{D}_n}{\theta}]. \quad (35)$$

Note that when $\dot{D}_n$ is absent, then

$$\kappa = \frac{\alpha}{\theta\beta}e^{b\theta(D_n-1)}(1 - e^{a\theta(D_n-1)}), \quad (36)$$

where

$$a = \frac{\beta}{\mu}|_{\dot{D}_n=0} = \frac{(\gamma+1)^2(\gamma-1)}{4\gamma^3}, \quad b = \frac{2}{c_s^2} - a = \frac{(\gamma+1)^3(3\gamma-1)}{4\gamma^3(\gamma-1)}, \quad (37)$$

and

$$\frac{\beta}{\alpha}|_{\dot{D}_n=0} = \frac{8(\gamma-1)^3}{(3-\gamma)(\gamma+1)^2}, \tag{38}$$

which agree with the *steady* ($\dot{D}_n = 0$) $D_n - \kappa$ relation established in [8]. Fig. 4. shows two representations of the $\dot{D}_n, D_n, \kappa$ - relation in the limit of large activation energy. The left plot shows a three dimensional representation of the surface in the $\dot{D}_n, D_n, \kappa$ - space, and the right plot shows $D_n - \kappa$ curves taken at different values of $\dot{D}_n$.

need a picture here, also need to comment about well-posedness, interesting properties and so on, bowtie, extended validity, equation tipe....

Fig. 4. Fig. 4. shows two representations of the $\dot{D}_n, D_n, \kappa$ - relation in the limit of large activation energy. The left plot shows a three dimensional representation of the surface in the $\dot{D}_n, D_n, \kappa$ - space, and the right plot shows $D_n - \kappa$ curves taken at different values of $\dot{D}_n$.

5 The Dynamics of a $\dot{D}_n, D_n, \kappa$ - Relation

Given that the asymptotic analysis suggest that the shock surface evolves according to a $\dot{D}_n, D_n, \kappa$ - relation, we discuss some of the changes to the numerics that are required in the level-set formulation, and illustrate some simple aspects of the changes in behavior that are observed from the dynamics of a D_n - κ - relation.

5.1 Numerical Methods

As in the original level-set method, if one consider the surface to a SPS, but one that obeys a relation of the type $F(\dot{D}_n, D_n, \kappa) = 0$, it is still the case that the level-set equation holds, i.e.

$$\frac{\partial \psi}{\partial t}|_{\mathbf{x}} + D_n|\nabla| = 0. \tag{39}$$

But now instead of having $D_n(\kappa)$, we have instead a relationship between the acceleration of the shock in the normal direction in terms of the normal velocity and curvature, $\dot{D}_n(D_n, \kappa)$. Note that it is possible to derive an additional kinematic relationship for $\dot{D}_n$. by taking its total derivative $\partial D_n/\partial t_{\mathbf{X}} + D_n \hat{n} \cdot \nabla = 0$, using the definition of the normal, $\hat{n} = \psi/|\psi|$ and one uses to derive an expression for the $\partial D_n/\partial t_{\mathbf{X}}$ that is needed for the numerics on the fixed grid

$$\frac{\partial D_n}{\partial t}|_{\mathbf{X}} = \dot{D}_n(D_n, \kappa), -D_n \frac{\nabla \psi}{|\nabla|} \cdot \nabla D_n. \tag{40}$$

Equations (39) and (40) are a set of two coupled, PDEs that are to solved simultaneously, for the evolution of the shock surface, for a give $\dot{D}_n, D_n, \kappa$ - relation. Notice that not only the initial position of the shock is needed, but also its initial velocity, as well.

5.2 Numerical Examples

Here we demonstrate numerically the differences between the evolution of a wave front governed by a $D_n - \kappa$ law and a $D_n - D_n dot - \kappa$ law. Experiment (a) is the numerical solution to the $D_n - \kappa$ problem, while experiment (b) is that of $D_n - D_n dot - \kappa$. We choose the initial wave to be at $x = .2(1 - cos(2\pi y))$, or equivalently a $\psi(x, y, t = 0) = x - .2(1 - cos(2\pi y))$. For experiment (b) we choose $D_n(x, y, t = 0) = 1$. The computational domain is $0 \leq x \leq 5$ and $0 \leq y \leq 1$, with continuation boundary conditions at $x = 0, 5$ and perfectly reflecting boundary conditions at $y = 0, 1$. For experiment (a) we take $D_n = 1 - .05\kappa$. For experiment (b) $D_n dot = -.025(D_n - 1) - .5\kappa$. Both relations allow for a flat non-accelerating wave to move with speed 1.

The results of the numerical experiment are shown in Figure 5. The dark lines are contours of the crossing table (i.e. location of waves at time intervals of 0.2), while the grey scale indicates the detonation normal velocity as the wave crosses a node point. Experiment (a) shows how the initial cosine wave smoothly evolves into a flat CJ wave, as expected by a wave governed by a $D_n - \kappa$ law. By contrast, experiment (b) starts out with smooth data, but in a short time the level-set function (and hence the wave shape) forms cusps and D_n becomes discontinuous. As the wave evolves further, these discontinuities reflect off the walls and demonstrate a cell-like pattern. This new phenomenon is due to the governing nonlinear hyperbolic PDE which governs the $D_n - D_n dot - \kappa$ relation. While this new relation is not a complete theory of cellular detonations, there is clearly similar features between the two.

need to comment on cells and revise

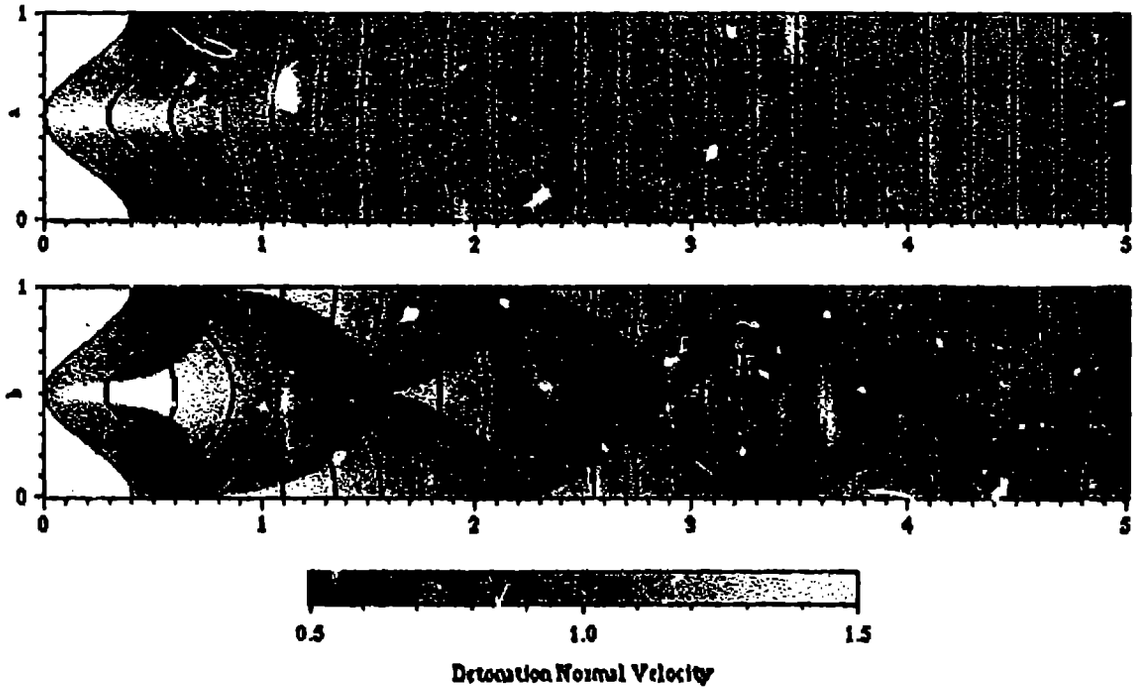

Fig. 5. An exampie of the comparison between the D-kappa relation and D-kappa-Dndot retlation

Acknowledgments

This work has been supported by the United States Air Force, Wright Laboratory, Armament Directorate, Eglin Air Force Base, F08630-92- K0057, and with computing resources from the National Center for Supercomputing Applications (NCSA). Tariq Aslam has partially been supported by an AASERT grant by AFOSR, Summer of 1994. D. S. Stewart had travel support from the National Science Foundation.

References

1. Osher, Stanley and Sethian, James, A., "Fronts Propagating with Curvature Dependent Speed: Algorithms Based on Hamilton-Jacobi Formulations", Journal of Computational Physics, 79, 12-49 (1988)
2. T. Aslam, J. Bdzil, and D. S. Stewart and "The level set method of Osher/Sethian Applied to Modeling Detonation Shock Dynamics", in preparation.
3. Yao, Jin and Stewart, D. Scott, "On the dynamics of detonation", to be submitted for publication.
4. Matalon, M. and Matkowsky, M., "Flames as gasdynamic discontinuities", J. Fluid Mech., vol. 124, pp., 239-259 (1982)

5. Buckmaster, J. and Ludford, G. S. S., *Theory of Laminar Flames*, Cambridge University Press, (1982), page 208.
6. Stewart, D. S. and Bdzil, J. B., "The shock dynamics of stable multi- dimensional detonation", Combustion and Flame, 72, 311-323 (1988).
7. Klein, R. and Stewart, D. S., "The relation between curvature and rate state-dependent detonation velocity", *SIAM Journal of Applied Mathematics*, in press, to appear, Oct 1993.
8. Yao, Jin and Stewart, D. S., "On the normal detonation shock velocity curvature relationship for materials with large activation energy.", to appear in *Combustion and Flame*.
9. Bdzil, J. B., Davis, W. C. and Critchfield, R. R. "Detonation Shock Dynamics (DSD) 'Calibration for PBX 9502' ", , Proceedings of the Tenth Symposium (International) on Detonation, Boston, Mass, 1993, to appear.
10. Private communication.
11. Bdzil, J. B., "Steady state two-dimensional detonation", Journal of Fluid Mechanics, Vol. 108, 1981, pp. 185-226.
12. Wood, W. W. and Kirkwood, J. G. "Diameter effects in condensed explosives: The relation between velocity and radius of curvature", *Journal of Chemical Physics*, 22: 1920-1924 (1954).
13. Klein, IMA article
14. Stewart, D. S. and Yao, Jin, "Critical Detonation Shock Curvature and Failure Dynamics: Developments in the Theory of Detonation Shock Dynamics", Development in Theoretical and Applied Mechanics, Volume XVII, page 204, (1994).
15. Bdzil, J. B. and Stewart, D. S., "Modeling of two- dimensional detonation with detonation shock dynamics", *Physics of Fluids*, A, Vol. 1, No. 7, 1261-, (1988).

6 junk

Figure 6. shows a schematic diagram of the typical edge angle evolution shown at different times t_1, t_2 and t_3, for a) an oblique shock/edge interaction and relaxation and b) for a normal shock/edge interaction. In case a) the detonatio shock is highly oblique relative to the edge and if the angle ω is below the sonic angle ω_s, the continuation boundary condition is applied. As the shock evolves the angle eventually obtains the sonic angle ω_s, where it is assumed that the reaction zone can be affected by confined. The boundary condition model then allows for a jump in ω to ω_c, which is characteristic of the explosive/confinement pair. Case b) shows a different case, where the shock is assumed to be highly normal to the edge, in which case the angle jumps from 90 degrees to ω_c. If the confinement is sufficiently weak, or thin, the angle jumps to the sonic angle ω_s, the sonic angle.

This article was processed using the LaTeX macro package with LMAMULT style